2011

Fibroblast growth factor 1 (FGFR1) modulation regulates repair capacity of oligodendrocyte progenitor cells following chronic demyelination

Yong-Xing Zhou
Uniformed Services University of the Health Sciences

Ravinder Pannu
Qiagen Inc.

Tuan Q. Le
Uniformed Services University of the Health Sciences

Regina C. Armstrong
Uniformed Services University of the Health Sciences, rarmstrong@usuhs.edu

Neurobiology of Disease xxx (2011) xxx–xxx

Contents lists available at SciVerse ScienceDirect

Neurobiology of Disease

journal homepage: www.elsevier.com/locate/ynbdi

Fibroblast growth factor 1 (FGFR1) modulation regulates repair capacity of oligodendrocyte progenitor cells following chronic demyelination

Yong-Xing Zhou [a], Ravinder Pannu [a,b], Tuan Q. Le [a], Regina C. Armstrong [a,*]

[a] Department of Anatomy, Physiology and Genetics, Uniformed Services University of the Health Sciences, Bethesda, MD USA
[b] Qiagen Inc., 6951 Executive Way, Frederick, MD USA

ARTICLE INFO

Article history:
Received 29 April 2011
Revised 24 July 2011
Accepted 3 August 2011
Available online xxxx

Keywords:
Oligodendrocyte
Progenitor
Regeneration
Remyelination
Fibroblast growth factor
Platelet-derived growth factor
Cuprizone
Differentiation
Demyelination
Multiple sclerosis
Axon damage

ABSTRACT

The adult mammalian brain contains multiple populations of endogenous progenitor cell types. However, following CNS trauma or disease, the regenerative capacity of progenitor populations is typically insufficient and may actually be limited by non-permissive or inhibitory signals in the damaged parenchyma. Remyelination is the most effective and simplest regenerative process in the adult CNS yet is still insufficient following repeated or chronic demyelination. Our previous in vitro studies demonstrated that fibroblast growth factor receptor 1 (FGFR1) signaling inhibited oligodendrocyte progenitor (OP) differentiation into mature oligodendrocytes. Therefore, we questioned whether FGFR1 signaling may inhibit the capacity of OP cells to generate oligodendrocytes in a demyelinating disease model and whether genetically reducing FGFR1 signaling in oligodendrocyte lineage cells could enhance the capacity for remyelination. FGFR1 was found to be upregulated in the corpus callosum during cuprizone mediated demyelination and expressed on OP cells just prior to remyelination. *Plp/CreER^T:Fgfr1$^{fl/fl}$* mice were administered tamoxifen to induce conditional *Fgfr1* deletion in oligodendrocyte lineage cells. Tamoxifen administration during chronic demyelination resulted in reduced FGFR1 expression in OP cells. OP proliferation and population size were not altered one week after tamoxifen treatment. Tamoxifen was then administered during chronic demyelination and mice were given a six week recovery period without cuprizone in the chow. After the recovery period, OP numbers were reduced and the number of mature oligodendrocytes was increased, indicating an effect of FGFR1 reduction on OP differentiation. Importantly, tamoxifen administration in *Plp/CreER^T:Fgfr1$^{fl/fl}$* mice significantly promoted remyelination and axon integrity. These results demonstrate a direct effect of FGFR1 signaling in oligodendrocyte lineage cells as inhibiting the repair capacity of OP cells following chronic demyelination in the adult CNS.

Published by Elsevier Inc.

Introduction

Optimization of the endogenous neural stem and progenitor cell capacity for repair of the adult CNS is a high priority among regenerative medicine approaches for diverse forms of CNS injury and disease. Remyelination is an excellent example of successful endogenous cell repair in the adult CNS and a relatively simple model for interrogating the cellular and molecular interactions that impact the effectiveness of regenerative responses from neural stem and progenitor cells. In the mammalian brain, endogenous neural stem cells of the subventricular zone and oligodendrocyte progenitor (OP) cells of the white matter can effectively generate new oligodendrocytes and exhibit extensive remyelination after a transient episode of demyelination (Aguirre et al., 2007; Murtie et al., 2005b; Nait-Oumesmar et al., 2008). However, with repeated or prolonged episodes of demyelination, OP cells become depleted and remyelination becomes less effective (Armstrong et al., 2006; Mason et al., 2004).

Growth factors, cytokines, and extracellular matrix molecules that can influence the regenerative responses of endogenous neural stem and OP cells can be associated with demyelination and the associated pathological features, such as reactive astrogliosis, microglia/macrophage activation, and inflammatory cell infiltration. Modifying the molecular signals of the lesion environment may attenuate inhibitory signals and promote endogenous cell regenerative responses. Our previous analyses of fibroblast growth factor 2 (FGF2), which is upregulated in areas of demyelination, have demonstrated proof-of-concept that genetic deletion of *Fgf2* can significantly improve spontaneous remyelination as well as reduce axonal damage associated with chronic demyelination (Armstrong et al., 2006, 2002; Tobin et al., 2011).

To better design approaches that can improve endogenous cell regenerative responses, it is important to identify the specific mechanisms of action and potential therapeutic targets. In vitro studies demonstrated a significant role of fibroblast growth factor receptor 1

* Corresponding author at: Department of Anatomy, Physiology and Genetics, Uniformed Services University of the Health Sciences, 4301 Jones Bridge Rd., Bethesda, MD 20814, USA. Fax: +1 301 295 1715.
E-mail address: rarmstrong@usuhs.edu (R.C. Armstrong).
Available online on ScienceDirect (www.sciencedirect.com).

0969-9961/$ – see front matter. Published by Elsevier Inc.
doi:10.1016/j.nbd.2011.08.004

(FGFR1) in mediating FGF2 inhibition of OP cell differentiation into oligodendrocytes (Zhou et al., 2006). The current studies evaluate FGFR1 expression corresponding with FGF2 upregulation in cuprizone induced demyelination of the corpus callosum (CC). We then use *Plp/CreER^T:Fgfr1$^{fl/fl}$* mice to test FGFR1 as a key component regulating oligodendrocyte lineage cell regenerative responses mediating remyelination. Cuprizone ingestion in mice produces reproducible and extensive demyelination, especially within the caudal CC (Wu et al., 2008; Xie et al., 2010), with pathological characteristics of oligodendrocyte loss that are shared with MS types III and IV (Liu et al., 2010; Lucchinetti et al., 1999). Cuprizone feeding can produce a prolonged period of experimental demyelination that models chronic demyelination effects including depletion of the OP cell population and inefficient spontaneous remyelination (Armstrong et al., 2006; Mason et al., 2004). Analysis of regenerative processes and remyelination is facilitated by the ability to remove the cuprizone demyelinating agent from the diet. Furthermore, use of the *Plp/CreER^T* construct provides conditional Cre recombinase expression to evaluate a direct effect of FGFR1 signaling in oligodendrocyte lineage cells and tamoxifen induction to target the FGFR1 gene deletion within the disease time course.

Materials and methods

Mice and cuprizone demyelination

All experimental procedures using mice were approved by the USUHS Institutional Animal Care and Use Committee. C57BL/6 mice were purchased from The Jackson Laboratory (Bar Harbor, ME). *Plp/CreER^T* mice (Doerflinger et al., 2003) were derived from breeding pairs purchased from The Jackson Laboratory (B6.Cg-Tg(Plp1-cre/ESR1) 3.16Pop/J; Bar Harbor, ME). Mice with a floxed *Fgfr1* allele were generated by Dr. Juha Partanan and provided through Dr. Flora Vaccarino (Yale University, New Haven, CT) (Pirvola et al., 2002). Mice with a floxed platelet-derived growth factor receptor alpha (*Pdgfrα*) allele were provided by Dr. Michelle Tallquist (Tallquist and Soriano, 2003). *Z/AP* dual reporter mice (Tg(CAG-Bgeo/ALPP)1Lbe/J; The Jackson Laboratory, Bar Harbor, ME) were provided by Dr. Tudor Badea (Johns Hopkins University, Baltimore, MD) (Lobe et al., 1999). All mouse lines were backcrossed to the C57BL/6 background. Male mice were fed *ad libitum* a diet of 0.2% (w/w) cuprizone (oxalic bis-(cyclohexylidenehydrazide); Sigma-Aldrich, Milwaukee, WI) mixed into milled chow pellets (Harlan Teklad, Madison, WI) beginning at 8 wks of age.

Expression analysis of FGF family of signaling components in C57BL/6 mice

Male C57BL/6 mice were analyzed at 8 wks of age prior to the start of cuprizone (0 wk), at 3-wk intervals throughout the 12-wk cuprizone treatment, or after a 6-wk recovery period. The CC was micro-dissected on ice, transferred to TRIZOL reagent (GIBCO-BRL, Grand Island, NY) and processed for RNA extraction. Following Turbo DNAse (Ambion, Foster City, CA) treatment to remove genomic DNA contamination, RNA samples from 3 mice per condition were pooled as template for cDNA synthesis using the RT2 First Strand cDNA synthesis kit (SABiosciences, Frederick, MD). For each time point cDNA was generated from 1.5 μg of RNA template (0.5 μg/mouse from each of 3 mice) and was run on triplicate plates. Gene expression was quantified using real-time PCR custom arrays with SYBR Green-optimized primers and internal controls for effective PCR reactions and genomic DNA contamination (SABiosciences) run on an ABI 7500 real time PCR cycler. Differences in the number of cycles to threshold (C_T) were analyzed using the $\Delta\Delta C_T$ method. Values were normalized to an average of housekeeping values obtained for the same samples run on a plate of 12 standardized housekeeping genes that included high and low abundance transcripts (SABiosciences; genes Actb, B2m, Gusb, Hsp90ab1, Ldhal6b, Nono, Ppia, Rpl13a, Tfrc, Tbp, Hprt1, Act1b, 18 s RNA). The average C_T values for this set of housekeeping genes ranged from 22.6 (0 wk, no cuprizone) to 23.8 (12 wk cuprizone plus 6 wk recovery), indicating relative stability across the disease time course. Fold changes in gene expression throughout the cuprizone time course were calculated relative to pre-treatment (0 wk) C_T values, with a detection threshold set at 35 cycles. Differential gene expression across the cuprizone time course and within the gene set was analyzed using Gene Pattern 2.0 software (Gould et al., 2006; Reich et al., 2006).

Detection of Cre recombinase activity using Z/AP dual reporter mice

Plp/CreER^T driven expression of Cre recombinase and the tamoxifen treatment protocol were tested by expression of alkaline phosphatase (AP) from recombination of the dual reporter in *Z/AP* mice. *PLP/CreER^T:Z/AP* mice were treated with tamoxifen at 4 wks of age, after the completion of developmental myelination, and sacrificed two weeks later for analysis of AP in coronal brain sections (Fig. 1A). Tamoxifen (4-hydroxytamoxifen; Sigma, St. Louis, MO) was administered by intraperitoneal injection (0.8 mg every 12 h for 5 days; total 8 mg). To eliminate endogenous AP activity tissue sections were incubated in PBS for heat inactivation (65 °C for 30 min) followed by incubation in levamisole for 10 min. AP reporter activity was detected using an NBT/BCIP (DAKO, Carpentaria, CA) substrate reaction.

Immunohistochemistry of Plp/CreER^T driven expression of Cre in oligodendrocytes

Transverse sections of spinal cord from *Plp/CreER^T* mice perfused at 6 wks of age were immunostained to confirm Cre expression in oligodendrocytes. Immunofluorescence for Cre (rabbit IgG polyclonal anti-Cre; Novagen, San Diego, CA) detected with goat anti-rabbit IgG Alexa Fluor 488 (Invitrogen, Carlsbad, CA) was combined with CC1 immunolabeling (mouse IgG monoclonal; Oncogene Research Products, Cambridge, MA) detected with donkey anti-mouse IgG F(ab)$_2$ fragment conjugated with Cy3 (Jackson ImmunoResearch).

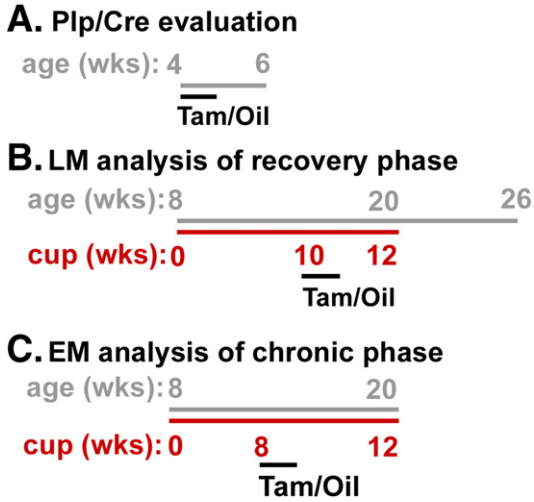

Fig. 1. Timing of tamoxifen treatment within experimental protocols. Mice were administered tamoxifen to induce nuclear translocation of the Cre recombinase fusion protein and subsequent deletion of floxed gene alleles. Different timing of tamoxifen administration was used to evaluate Cre activity driven from the proteolipid protein (PLP) gene promoter (A), for light microscopic (LM) analysis of chronic demyelination and recovery (B) and for electron microscopic analysis (EM) of during chronic demyelination. Tamoxifen was administered by intraperitoneal injections of 0.8 mg every 12 h for 5 days with a total dose of 8 mg. Cuprizone feeding began at 8 wks of age and continued for up to 12 wks, i.e. 20 wks of age. Lines are not drawn to scale for specific number of wks shown by numbers.

Please cite this article as: Zhou, Y.-X., et al., Fibroblast growth factor 1 (FGFR1) modulation regulates repair capacity of oligodendrocyte progenitor cells following chronic demy..., Neurobiol. Dis. (2011), doi:10.1016/j.nbd.2011.08.004

Tamoxifen induction of conditional deletion of Fgfr1or Pdgfrα

Tamoxifen treatment was used to induce conditional deletion of *Fgfr1* in oligodendrocyte lineage cells of *Plp/CreER^T:Fgfr1$^{fl/fl}$* mice or *Pdgfrα* in *Plp/CreER^T:Pdgfrα$^{fl/fl}$* mice. Tamoxifen was administered, as noted above for *Z/AP* mice, starting on week 8 or week 10 of cuprizone treatment (Figs. 1B, C). Control mice of the same genotype were administered sunflower oil vehicle only. For analysis of cell proliferation, mice were given two injections of bromodeoxyuridine (BrdU; Sigma, 200 mg/kg i.p.), each 2 h apart, and sacrificed at the end of the four-hour period for BrdU incorporation, as previously detailed (Armstrong et al., 2002). Mice were perfused with 3% paraformaldehyde for immunohistochemistry and in situ hybridization of coronal brain sections. FGFR1 was detected using a mouse monoclonal FGFR1 antibody clone 19B2 (Upstate Biotech., Lake Placid, NY). PDGFαR, NG2, CC1 and myelin oligodendrocyte glycoprotein (MOG) immunolabeling were performed as previously detailed (Armstrong et al., 2006; Murtie et al., 2005b). Preparation of digoxigenin labeled riboprobes for PLP and PDGFαR and in situ hybridization with detection by reaction in NBT/BCIP substrate (DAKO, Carpinteria, CA) along with BrdU detection was performed as previously detailed (Armstrong et al., 2002; Redwine and Armstrong, 1998).

Images of in situ hybridization and immunostaining results were captured with a Spot 2 CCD digital camera using Spot Advanced image acquisition software (Diagnostic Instruments, Sterling Heights, MI). Images were prepared as panels using Adobe Photoshop 7 (San Jose, CA). Quantification of immunohistochemistry and in situ hybridization results included at least 3 sections per mouse and 3 mice per condition. As previously reported (Armstrong et al., 2002), OP cells were counted and areas measured using Spot software, cells expressing PLP mRNA were quantified using unbiased stereologic morphometric analysis, and MOG immunolabeling was quantified using pixel thresholding of myelinated areas using Metamorph software (Molecular Devices, Downingtown, PA).

Ultrastructural analysis of myelin and axon pathology

Following treatment with cuprizone and tamoxifen (Fig. 1C), mice were perfused with 2% paraformaldehyde/3% acrolein for processing of parasagittal sections for electron microscopy and for alternate sections to be process for immunohistochemistry, as previously described (Xie et al., 2010). Cuprizone pathology differs along the rostro-caudal extent of the CC with the most extensive pathology observed in the caudal CC (Wu et al., 2008; Xie et al., 2010). Therefore, analyses focused on the caudal CC (−1.5 to −2.0 mm relative to bregma) (Xie et al., 2010). Sections were examined in a Philips CM100 transmission electron microscope and images were imported into MetaMorph (Molecular Devices, Downington, PA) for quantitative analysis, including axon diameter and myelin thickness. Myelin thickness was calculated from the average of radial measurements at 4 points per sheath, avoiding areas of tongue processes or fixation artifact. Axons diameters were calculated from measurement of the axon circumference. Axons with diameters typical of unmyelinated fibers (<0.3 μm) were excluded from analysis in order to more specifically follow the changes associated with demyelination and remyelination within the myelinated fiber population (Mason et al., 2001; Tobin et al., 2011; Xie et al., 2010).

Immunohistochemical analysis of axon integrity

Alternate tissue sections were processed for electron microscopy (above) or immunohistochemistry. Parasagittal floating 40 μm sections were double-immunostained for total neurofilament (NF200, rabbit polyclonal pan-neurofilament antibody, Chemicon, Billerica, MA) and non-phosphorylated neurofilament (SMI-32, mouse monoclonal IgG; Covance) to evaluate axonal integrity (Tobin et al., 2011). NF200-positive and SMI-32-positive cross-sectional profiles were counted on high magnification images acquired on a Zeiss Pascal confocal microscope with a 63× objective and then imported into Adobe Photoshop 7. Axonal damage was estimated as the percentage of SMI-32-positive profiles among all neurofilament-positive profiles counted.

Statistical analysis

Prism (Graph Pad Software) was used for statistical analyses and production of graphs. Across cuprizone time points, values for a single mouse genotype were examined using one-way ANOVA whereas two genotypes were compared using two-way ANOVA. For gene expression pattern analysis, one-way ANOVA across cuprizone stages was followed by analysis of each time point with a one sample *t*-test comparison to a theoretical mean of 1.000 (i.e. no fold change). Values of two genotypes or conditions at a single time point were compared using a *t*-test. Scattergraph data was analyzed by linear regression and comparison of the slopes and intercepts. A level of 0.05 was used for the overall test of significance. Values are expressed as the mean ± standard error of the mean.

Results

Expression pattern of FGF family of ligands and receptors throughout the cuprizone disease time course

Quantitative RT-PCR custom arrays of the FGF family, along with selected markers of distinct cell types, were used to examine expression and potential relevance to FGF signaling throughout the course of cuprizone demyelination and recovery. Genes expressed in reactive astrocytes, microglia/macrophages, and OP cells increase during demyelination and separate into a distinct hierarchal cluster from genes that decrease with cuprizone induced loss of oligodendrocytes and myelin (Fig. 2; Table 1). The appropriate hierarchical clustering of cell type specific markers demonstrates fidelity of the processing and analysis methods for detecting expression changes throughout the disease course (Fig. 2; gray). FGFR1, FGF2, and FGF12 align within the cluster of markers for astrocytes, microglia, and OP cells indicating potential expression in reactive cell types in contrast to mature oligodendrocytes. Alignment of FGFR1 within the same cluster as FGF2 is supportive of FGFR1 as relevant to FGF2 signaling in this context (Fig. 2; yellow cluster). Although FGF12 also falls within the FGFR1 cluster, FGF12 acts independently of FGFRs and therefore is not a relevant partner for FGFR1 (Itoh and Ornitz, 2008). Several FGF family ligands (FGF4, 6, 14–16, 21) did not rise above the detection threshold at any time points (not shown).

FGFR1 regulation of recovery following chronic demyelination

Plp/CreER^T mice were crossed with floxed alleles of *Fgfr1* to directly examine the role of FGFR1 in OP cells and the generation of oligodendrocytes during remyelination. The *Plp/CreER^T* mouse design employs tamoxifen administration to induce deletion of floxed alleles at desired stages of chronic disease progression to minimize the potential for compensatory effects during development or earlier stages of disease. Effectiveness of the tamoxifen procedure and dose for induction of Cre translocation and recombination in cells contributing to myelination was demonstrated using *Plp/CreER^T:Z/AP* reporter mice (Fig. 3A). Localization of Cre protein in oligodendrocytes was confirmed by immunohistochemical co-localization with CC1 (Figs. 3B–D). Although PLP promoter activity is highest in mature oligodendrocytes, sufficient expression in *Plp/CreER^T* mice to drive effective recombination in OP cells was demonstrated when crossed to floxed *Pdgfrα* mice. Tamoxifen administration (Fig. 1A) resulted in

Please cite this article as: Zhou, Y.-X., et al., Fibroblast growth factor 1 (FGFR1) modulation regulates repair capacity of oligodendrocyte progenitor cells following chronic demy..., Neurobiol. Dis. (2011), doi:10.1016/j.nbd.2011.08.004

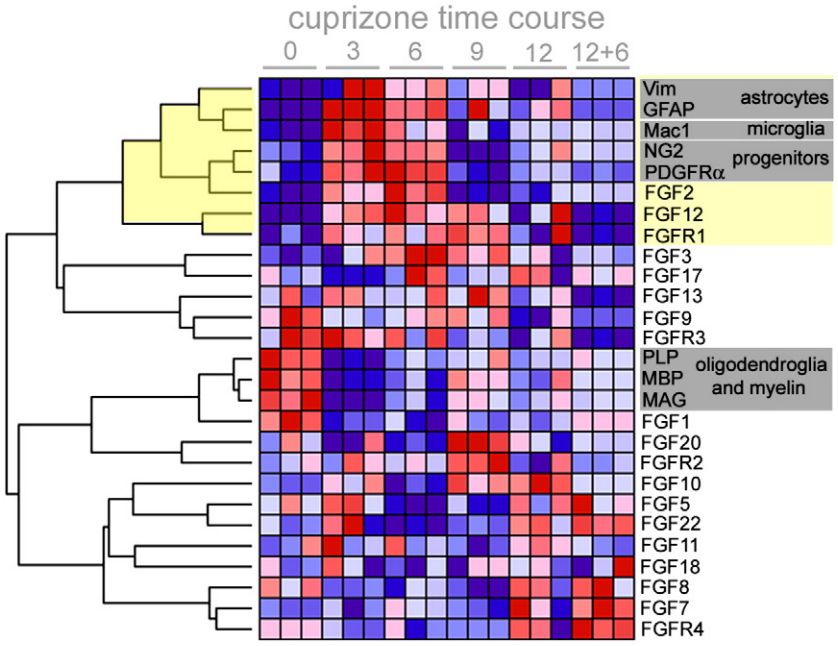

Fig. 2. Expression profile for FGF family of ligands and receptors throughout the course of cuprizone demyelination and recovery. Heat map to show differential gene expression following quantitative RT-PCR of RNA isolated from the CC of C57BL/6 mice at intervals noted throughout the cuprizone treatment and recovery periods. For each gene the lowest values are represented by dark blue and progressing through light blue and pinks to reds for the highest values. Columns show results of technical triplicates run on separate plates for each time point (N = 3 mice per time point). Genes that are characteristic of distinct cellular response are noted (gray highlights). Associations among gene patterns across the disease time course are identified by heirarchical cluster analysis. Genes that align within the heirarchical cluster corresponding with FGF2 (yellow highlights) have values of fold increases and statistical comparisons shown in Table 1.

a 35% reduction of PDGFαR expression among NG2 cells in *Plp/CreER*^{T}:*Pdgfrα*$^{fl/fl}$ mice ($p = 0.0002$; Fig. 3E).

Next, expression of FGFR1 in the CC of chronically demyelinated mice was confirmed by immunohistochemistry (Fig. 4). Of importance relative to the potential to regulate remyelination, FGFR1 was expressed among OP cells identified by NG2 immunolabeling in the CC of mice at 12 wks of cuprizone treatment prior to the recovery phase (Figs. 4A–C). To reduce FGFR1 expression at this corresponding period, *Plp/CreER*^{T}:*Fgfr1*$^{fl/fl}$ mice were administered tamoxifen or oil (vehicle) after 10 wks of cuprizone and continued on cuprizone through 12 wks prior to perfusion (Fig. 1B). Tamoxifen treatment resulted in a 33% reduction of FGFR1 expression among NG2 cells in the chronically demyelinated CC as compared to vehicle-treated mice ($p = 0.0105$; Fig. 4D). In these mice, the OP population was also identified by in situ hybridization for PDGFαR and proliferation was examined by BrdU incorporation during a 4-h terminal pulse at the end of the 12 wks of cuprizone (Figs. 4E–F). Proliferation of OP cells was not significantly altered with tamoxifen treatment ($p > 0.05$; Fig. 4F). In addition, tamoxifen treatment did not significantly change the number of OP cells in *Plp/CreER*^{T}:*Fgfr1*$^{fl/fl}$ mice examined after 12 wks of cuprizone (Fig. 4G). However, when a 6-wk recovery period was added after 12 wks of cuprizone, the OP population was reduced in the tamoxifen treated mice as compared to controls ($p < 0.05$; Fig. 4G). Over this 6-wk recovery period, the reduced OP population could result from decreased OP proliferation or an increase of OP cells differentiating into mature oligodendrocytes.

The role of FGFR1 in the oligodendrocyte lineage during the recovery from demyelination was further examined using in situ hybridization for PLP to identify oligodendrocytes and immunohistochemistry for MOG to estimate the extent of remyelination (Fig. 5). *Plp/CreER*^{T}:*Fgfr1*$^{fl/fl}$ mice were administered tamoxifen or oil (vehicle) starting after 10 wks of cuprizone, continued on cuprizone through 12 wks, and then allowed a 6-wk recovery period on normal chow prior to perfusion (Fig. 1B). In situ hybridization for PLP mRNA

Table 1
Quantitative RT-PCR of cell type markers and signaling components clustered with FGF2.

Gene	0 wk No cup	3 wk cup	6 wk cup	9 wk cup	12 wk cup	12 wk cup 6 wk off	ANOVA p value
Vim	1.04 ± 0.22	46.22 ± 11.78	17.45* ± 2.18	10.92* ± 1.40	5.52 ± 3.39	0.24 ± 0.14	0.0003
GFAP	1.08 ± 0.30	41.39* ± 4.81	19.81* ± 2.26	11.53 ± 3.04	9.82 ± 2.10	0.12 ± 0.04	<0.001
Mac1	1.00 ± 0.03	49.09* ± 7.76	15.02* ± 1.09	5.81 ± 1.27	7.09* ± 1.02	1.32* ± 0.07	<0.001
NG2	1.02 ± 0.14	9.41* ± 0.19	5.00* ± 0.56	0.60 ± 0.09	2.20 ± 0.48	0.87 ± 0.00	<0.001
PDGFRα	1.03 ± 0.19	6.40* ± 0.57	4.22* ± 0.32	0.94 ± 0.17	1.25 ± 0.11	0.25 ± 0.00	<0.001
FGF2	1.00 ± 0.00	16.29* ± 3.07	15.06* ± 0.54	2.18* ± 0.15	3.51 ± 0.59	2.42 ± 0.00	<0.001
FGF12	1.02 ± 0.16	7.77* ± 0.18	5.64* ± 0.70	3.87* ± 0.34	3.31 ± 1.48	0.29* ± 0.11	<0.001
FGFR1	1.07 ± 0.29	3.51 ± 0.72	2.34 * ± 0.23	2.56* ± 0.35	2.01 ± 0.78	0.50 ± 0.00	0.0107
MBP	1.04 ± 0.21	0.07* ± 0.02	0.14* ± 0.04	0.34* ± 0.05	0.18* ± 0.17	0.03* ± 0.01	0.0005
PLP	1.02 ± 0.15	0.15* ± 0.03	0.26* ± 0.05	0.28* ± 0.09	0.13* ± 0.01	0.12* ± 0.00	<0.001
MAG	1.02 ± 0.14	0.12* ± 0.02	0.17* ± 0.02	0.24* ± 0.02	0.14* ± 0.03	0.02* ± 0.01	<0.001

Values shown are fold change (mean ± s.e.m.) calculated relative to 0 wk No cuprizone condition. N = 3 mice per condition with samples run across 3 plates as technical triplicates. ANOVA values are for comparison across all time points for a given gene. Asterisks show significant changes ($p < 0.05$) for individual time points using a one sample *t*-test comparison to a theoretical mean of 1.000, i.e. null hypothesis for no fold change.

Please cite this article as: Zhou, Y.-X., et al., Fibroblast growth factor 1 (FGFR1) modulation regulates repair capacity of oligodendrocyte progenitor cells following chronic demy..., Neurobiol. Dis. (2011), doi:10.1016/j.nbd.2011.08.004

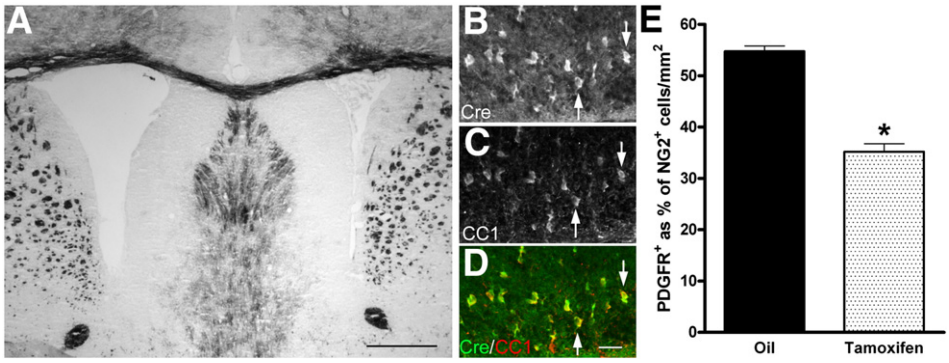

Fig. 3. *Plp/CreER^T* line applicability across stages of the oligodendrocyte lineage. *Plp/CreER^T* mice were crossed to *Z/AP* reporter mice (A) or floxed *Pdgfrα* mice (B–E), administered tamoxifen at 4 wks of age, and perfused at 6 wks of age (see Fig. 1A). *Plp/CreER^T:Z/AP* mice demonstrate recombination and alkaline phosphatase (AP) reporter localization in myelinated tracts (A). Immunohistochemistry within white matter from *Plp/CreER^T:Pdgfrα$^{fl/fl}$* mice shows co-localization (arrows show two examples) of Cre recombinase protein in oligodendrocytes identified by CC1 antibody (B–D). Quantification of immunohistochemistry shows that tamoxifen administration in *Plp/CreER^T:Pdgfrα$^{fl/fl}$* mice reduces co-expression of PDGFαR among oligodendrocyte progenitors, identified by NG2 immunolabeling (E, $p = 0.0002$, $N = 3$ mice of each condition). Scale bar = 500 μm (A) and 25 μm (D).

transcripts showed significant reduction of oligodendrocytes in the CC of mice receiving either tamoxifen or oil after 12 wks of cuprizone ($p<0.001$; Figs. 5A–C), indicating similar oligodendrocyte loss. Furthermore, immunohistochemistry for myelin oligodendrocyte glycoprotein (MOG) to detect myelinated areas indicated similar demyelination at 12 wks of cuprizone ($p<0.001$ compared to no cuprizone; Figs. 5D–F). After the 6-wk recovery period, tamoxifen treated mice exhibited extensive repair capacity based on both recovery of oligodendrocytes ($p>0.05$ vs no cuprizone; Figs. 5A–C) and normalization of MOG values ($p>0.05$ vs no cuprizone; Figs. 5D–F). In contrast, after the 6-wk period on normal chow, vehicle-treated mice continued to exhibit oligodendrocyte loss ($p<0.001$ vs no cuprizone;

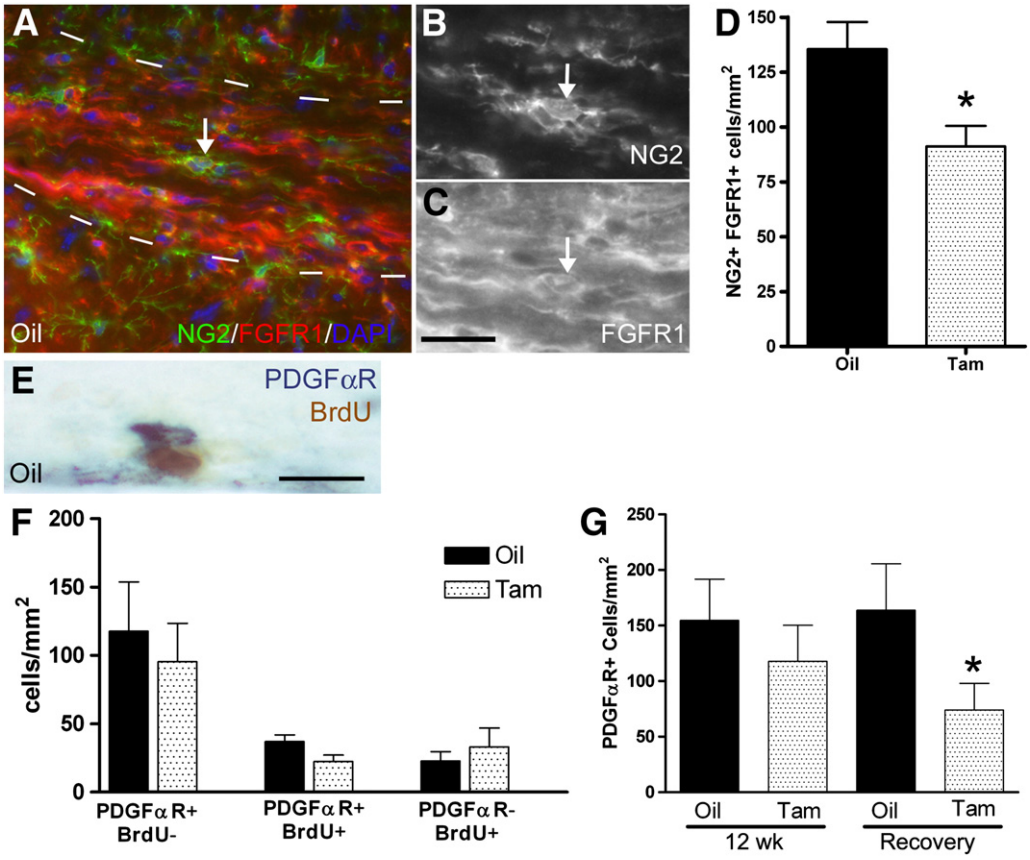

Fig. 4. Reduction of FGFR1 expression in oligodendrocyte progenitor (OP) cells. Analysis of coronal sections of corpus callosum from *Plp/CreER^T:Fgfr1$^{fl/fl}$* mice administered tamoxifen (Tam) or vehicle (Oil) after 10 wks of cuprizone (see Fig. 1B) and then perfused at the end of 12 wks of cuprizone (A–G) or after a 6-wk recovery period without cuprizone in the diet (G). Arrow indicates OP cells identified by NG2 immunolabeling (A, green; B) with co-localization of FGFR1 (A, red; C) in the corpus callosum (outlined by dash marks in A) after 12 wks of cuprizone in mice administered oil. FGFR1 expression is reduced among NG2 cells in mice administered tamoxifen compared with oil (D, $p = 0.0105$, $N = 5$ mice of each condition). Example of OP cells, identified by in situ hybridization for PDGFαR (blue-black NBT-BCIP substrate) combined with immunostaining for BrdU (brown DAB substrate) incorporated during a 4-h terminal pulse at 12 wks of cuprizone (E; oil control mouse shown). Tamoxifen treatment does not significantly alter the population of PDGFαR + cells labeled with BrdU at 12 wks of cuprizone (F). Quantification of total PDGFαR + cells after 12 wks of cuprizone (12 wk) or after 12 wks of cuprizone followed by a 6-wk recovery period (Recovery). Tamoxifen treated mice showed a reduction of total OP cells only after the recovery period (G; $p<0.05$ for tamoxifen versus oil after 12 wks of cuprizone and 6 wks on normal chow; $N = 5$ mice of each condition for both 12 wk and recovery time points). Scale bars = 25 μm for A–C (shown in C) and for E.

Please cite this article as: Zhou, Y.-X., et al., Fibroblast growth factor 1 (FGFR1) modulation regulates repair capacity of oligodendrocyte progenitor cells following chronic demy..., Neurobiol. Dis. (2011), doi:10.1016/j.nbd.2011.08.004

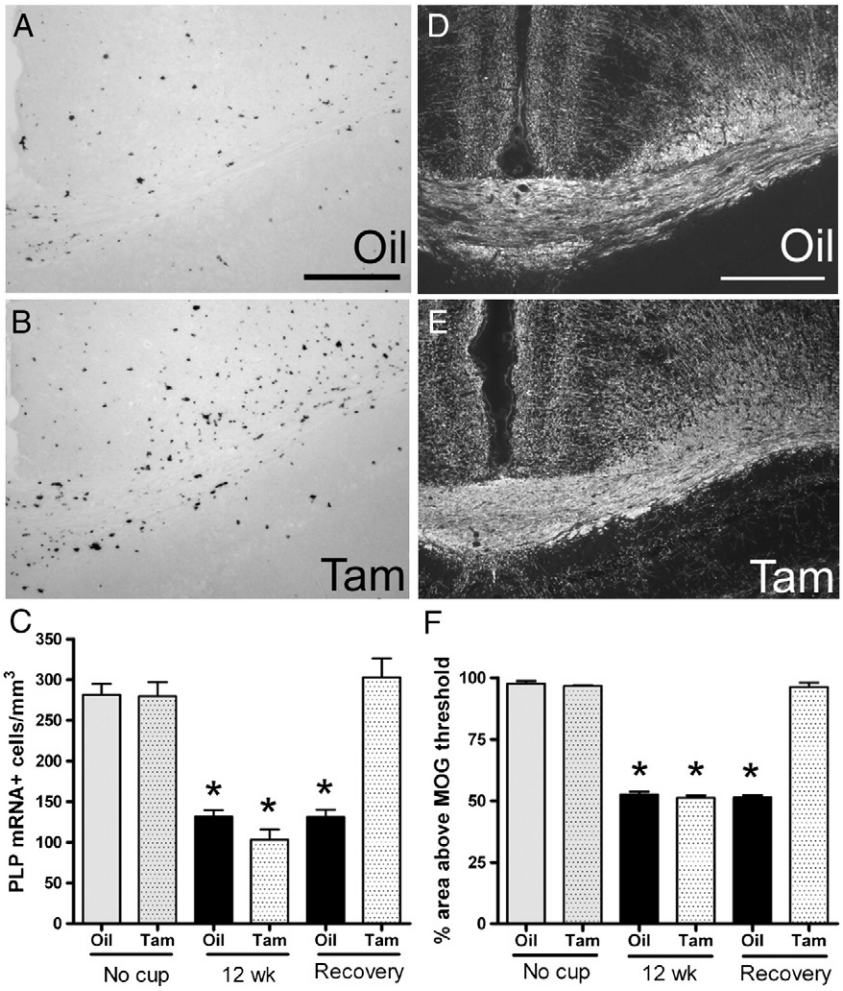

Fig. 5. Reduced FGFR1 expression increases oligodendrocyte repopulation of lesions and promotes remyelination following chronic demyelination. *Plp/CreER^T:Fgfr1$^{fl/fl}$* mice were administered vehicle (Oil; A, D) or tamoxifen (Tam; B, E) after 10 wks of cuprizone and then perfused at the end of 12 wks of cuprizone or after a 6-wk recovery period without cuprizone in the diet (see Fig. 1B). Images of coronal sections through the CC showing oligodendrocytes (A, B), identified by in situ hybridization for proteolipid protein (PLP) and myelin (D, E), immunostained for myelin oligodendrocyte glycoprotein (MOG), in mice perfused after 12 wks of cuprizone followed by 6 wks on normal chow. Quantification of oligodendrocytes in the CC using unbiased stereology (C; N = 3–4 mice per condition). Oligodendrocyte loss is significant in both tamoxifen and oil treated mice (*$p<0.001$ vs no cuprizone for each condition). During the recovery period, tamoxifen treated mice show enhanced repopulation of lesion areas ($p>0.05$ vs no cuprizone) as compared to vehicle controls (*$p<0.001$ vs no cuprizone)). The percent area of the CC with MOG immunoreactivity above threshold (based on non-demyelinated dorsal fornix) serves as an estimate of the myelinated area (F; N = 3 mice per condition). Mice administered tamoxifen or oil shows similar extents of demyelination after 12 wks of cuprizone (F, *$p<0.001$ vs no cuprizone, N = 3 mice of each condition). During the recovery period after chronic demyelination, mice administered tamoxifen have a significant improvement with normalization of the myelinated area ($p>0.05$ vs. no cuprizone) as compared to the continued presence of demyelinated area in the vehicle controls (*$p<0.01$ vs no cuprizone). Scale bars in A, D = 250 μm.

Figs. 5A–C) and chronic demyelination ($p<0.001$ vs no cuprizone; Figs. 5D–F). This difference in MOG immunolabeling after the 6-wk recovery indicates differential remyelination and is not the result of less demyelination having occurred since both tamoxifen and oil treated mice have approximately 50% of the CC area immunolabeled for MOG at the end of the 12 wks of cuprizone (Fig. 5F). These findings demonstrate that reduced expression of FGFR1 resulted in enhanced oligodendrocyte repopulation and remyelination in the CC following chronic demyelination.

Ultrastructural analysis of FGFR1 impact on myelin and axons during chronic demyelination

To further explore the potential role of FGFR1 at the earliest stages of remyelination, *Plp/CreER^T:Fgfr1$^{fl/fl}$* mice were treated with tamoxifen at 8 wks of cuprizone, continued on cuprizone through 12 wks and then perfused for electron microscopy (Figs. 1C, 6A–B). This protocol allows examination of a cycle of OP proliferation and repopulation that occurs during the late stage of continued cuprizone treatment even before returning the mice to normal chow (Armstrong et al., 2006; Mason et al., 2004). In addition, electron microscopy can detect enhanced remyelination at an earlier stage than MOG immunolabeled area measurements (Tobin et al., 2011). In wild type mice that have not been treated with cuprizone, approximately 80% of axons over 0.3 μm in diameter are myelinated in the caudal CC, as we have previously reported (Tobin et al., 2011) and confirmed in *Plp/CreER^T:Fgfr1$^{fl/fl}$* mice (82.75 ± 1.46). Axons with diameters less than 0.3 μm may involve unmyelinated axons and so are excluded. In *Plp/CreER^T:Fgfr1$^{fl/fl}$* mice prepared as in Fig. 1C, the proportion of myelinated axons is increased to almost 60% in tamoxifen treated mice as compared to less than 20% in *Plp/CreER^T:Fgfr1$^{fl/fl}$* mice administered oil ($p<0.0001$; Fig. 6E). A reduced slope in the relationship of myelin thickness to axon diameter (Fig. 6G) is indicative of a significant population of remyelinated fibers. The tamoxifen treated *Plp/CreER^T:Fgfr1$^{fl/fl}$* mice show a significantly reduced slope (0.028 ± 0.002) indicative of remyelination when compared to mice administered oil (0.054 ± 0.004; $p<0.0001$) or control *Plp/CreER^T:Fgfr1$^{fl/fl}$* mice that were not fed cuprizone (0.046 ± 0.009; $p = 0.013$). In contrast, the myelinated fibers remaining in the

Please cite this article as: Zhou, Y.-X., et al., Fibroblast growth factor 1 (FGFR1) modulation regulates repair capacity of oligodendrocyte progenitor cells following chronic demy..., Neurobiol. Dis. (2011), doi:10.1016/j.nbd.2011.08.004

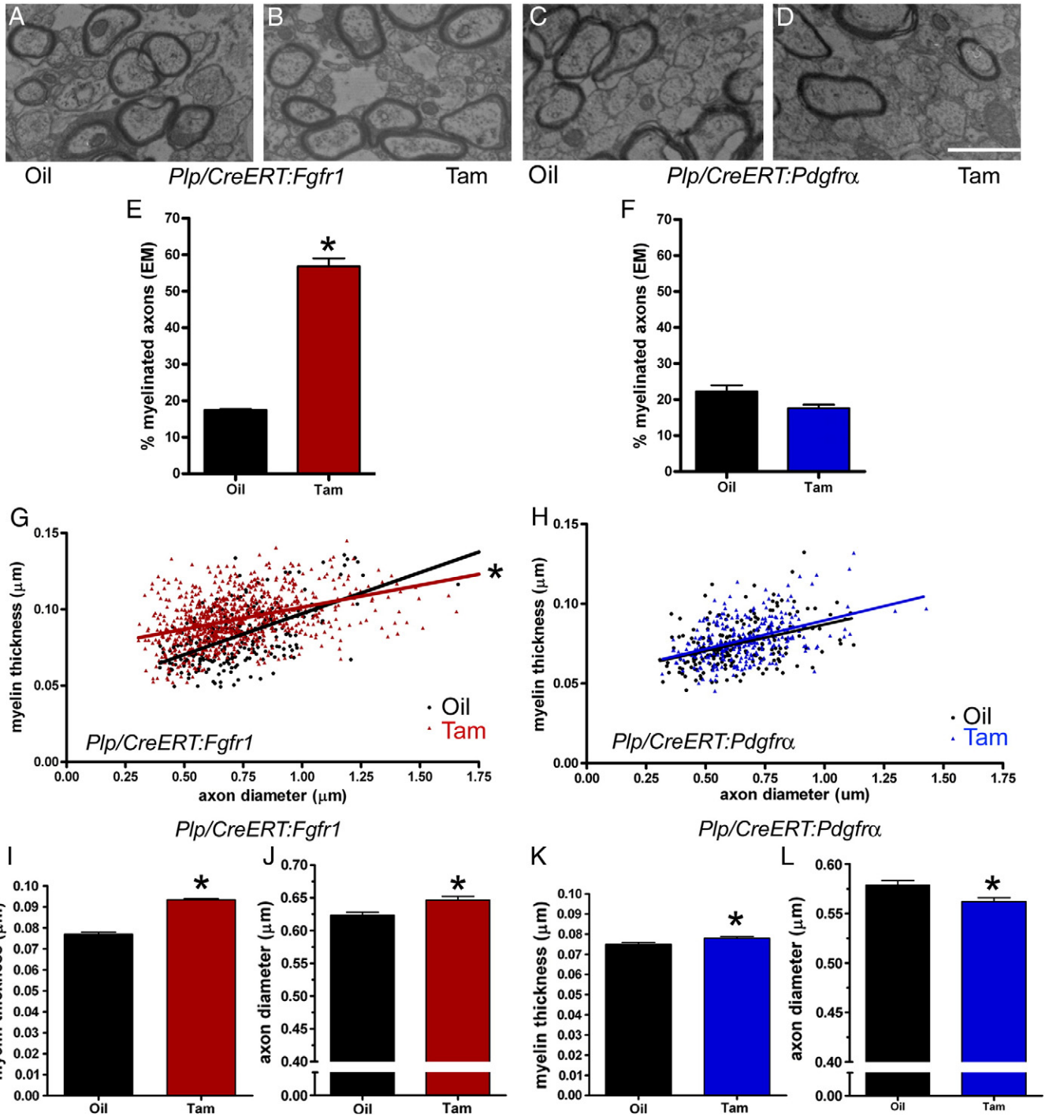

Fig. 6. Ultrastructural analysis of myelin and axons during chronic cuprizone treatment in *Plp/CreER^T:Fgfr1$^{fl/fl}$* mice with comparison to *Plp/CreER^T:Pdgfrα$^{fl/fl}$* mice. Mice were administered tamoxifen (Tam) or vehicle (Oil) after 8 wks of cuprizone and then perfused at the end of 12 wks of cuprizone treatment (Fig. 1C). Electron micrographs of *Plp/CreER^T:Fgfr1$^{fl/fl}$* mice administered oil (A) or tamoxifen (B) and *Plp/CreER^T:Pdgfrα$^{fl/fl}$* mice administered oil (C) or tamoxifen (D). Quantification of myelin and axon parameters in *Plp/CreER^T:Fgfr1$^{fl/fl}$* mice (E, G, I, J) or *Plp/CreER^T:Pdgfrα$^{fl/fl}$* mice (F, H, K, L). The percent myelinated axons is significantly greater in *Plp/CreER^T:Fgfr1$^{fl/fl}$* mice administered tamoxifen (E, $p<0.001$, similar results in each of two cohorts for total of $N=6$ for Oil and $N=7$ for Tam). The slope of myelin thickness relative to axon diameter is significantly reduced in *Plp/CreER^T:Fgfr1$^{fl/fl}$* mice administered tamoxifen (G, $p<0.001$). Overall mean values of both myelin thickness and axon diameter are increased in *Plp/CreER^T:Fgfr1$^{fl/fl}$* mice administered tamoxifen (I, $p<0.001$; J, $p=0.0018$). The percent myelinated axons is not significantly different for *Plp/CreER^T:Pdgfrα$^{fl/fl}$* mice treated with oil or tamoxifen ($p=0.614$; $N=4$ mice of each condition). Overall mean values of myelin thickness are slightly higher with tamoxifen treatment in *Plp/CreER^T:Pdgfrα$^{fl/fl}$* mice (K, $p=0.0188$) while axon diameters are decreased (L, $p=0.0058$). Scale bar = 1 μm.

oil treated mice probably were never demyelination based on the similarity of the slope to that of the mice which were not fed cuprizone. Average axon diameters were increased in the *Plp/CreER^T:Fgfr1$^{fl/fl}$* mice administered tamoxifen, indicating a potential benefit of remyelination to axon integrity ($p=0.0018$; Fig. 6J).

Analysis of Plp/CreER^T:Pdgfrα$^{fl/fl}$ mice demonstrates specificity of FGFR1 effect

Plp/CreER^T:Pdgfrα$^{fl/fl}$ mice were tested for expected differential effects from *Plp/CreER^T:Fgfr1$^{fl/fl}$* mice. PDGFαR is expressed on OP cells,

including OP cells that continue to proliferate after 12 wks of cuprizone (Figs. 4E, F). *Pdgfrα* haploinsufficiency results in reduced oligodendrogenesis during remyelination from cuprizone (Murtie et al., 2005b), which would be counter to the current results in *Plp/CreER^T:Fgfr1$^{fl/fl}$* mice (Fig. 5). In *Plp/CreER^T:Pdgfrα$^{fl/fl}$* mice, approximately 20% of axons were myelinated in mice administered either tamoxifen or oil ($p = 0.614$; Fig. 6F). The quantification of axon and myelin parameters in the *Plp/CreER^T:Pdgfrα$^{fl/fl}$* mice is consistent with a low proportion of remyelinated fibers (Fig. 6 H, K, L). This result clearly demonstrates that tamoxifen treatment during chronic demyelination in *Plp/CreER^T:Pdgfrα$^{fl/fl}$* mice (Fig. 6F) did not have the same effect on remyelination as was observed in *Plp/CreER^T:Fgfr1$^{fl/fl}$* mice (Fig. 6E). Furthermore, the results show that values in the oil treated condition of both *Plp/CreER^T:Pdgfrα$^{fl/fl}$* mice and *Plp/CreER^T:Fgfr1$^{fl/fl}$* mice are fairly similar (Figs. 6E, F) which supports the distinction of an effect of FGFR1 deletion with tamoxifen administration.

Analysis of neurofilament dephosphorylation as an indicator of axon damage

Chronic cuprizone demyelination results in axon damage which can be evaluated by ultrastructural analysis (Fig. 6) and more readily quantified by immunohistochemical detection of dephosphorylated neurofilaments (Xie et al., 2010; Tobin et al., 2011). To examine the effect of FGFR1 on axon damage in conjunction with the effects on remyelination, *Plp/CreER^T:Fgfr1$^{fl/fl}$* mice were administered tamoxifen or oil at 8 wks of cuprizone, continued on cuprizone through 12 wks and then perfused (Fig. 1C). Parasagittal sections of the corpus callosum were double immunolabeled for SMI32 (dephosphorylated neurofilaments indicative of damaged axons) and for NF200 (neurofilaments regardless of phosphorylation state indicative of total axon population) (Fig. 7). *Plp/CreER^T:Fgfr1$^{fl/fl}$* mice administered oil showed a marked proportion of axons immunolabeled for SMI32 which is consistent with our previous studies of wild type mice (Xie et al., 2010; Tobin et al., 2011). In contrast, *Plp/CreER^T:Fgfr1$^{fl/fl}$* mice administered tamoxifen showed over a 44% reduction in the proportion of SMI32 immunolabeled axons. This significant ($p = 0.0207$) difference indicated attenuation of axon damage during chronic demyelination associated with tamoxifen deletion of *Fgfr1* in oligodendrocyte lineage cells.

Discussion

The current study identifies FGFR1 as a key component regulating remyelination. Tamoxifen-induced reduction of FGFR1 expression in OP cells that persist during chronic demyelination resulted in enhanced oligodendrogenesis and remyelination. Electron microscopy confirmed that a greater proportion of demyelinated axons underwent spontaneous remyelination in *Plp/CreER^T:Fgfr1$^{fl/fl}$* mice administered tamoxifen. Corresponding changes in the OP cell population relative to the oligodendrocyte population, in the absence of changes in BrdU labeling, indicate that FGFR1 impacts remyelination through regulating OP differentiation and not through modulation of OP proliferation. Furthermore, reduction of FGFR1 expression in oligodendrocyte lineage cells reduced the extent of axon damage which demonstrates a significant positive effect of oligodendrogenesis and remyelination on axon integrity in a model of chronic demyelination.

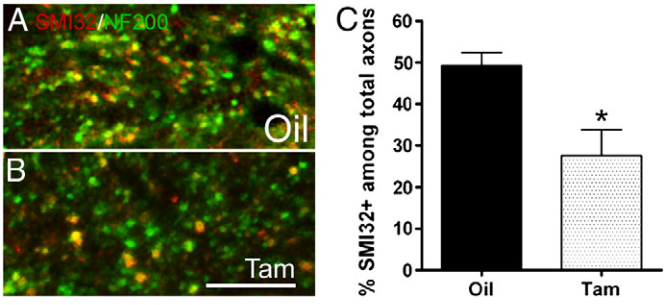

Fig. 7. Analysis of axon damage during chronic cuprizone treatment in *Plp/CreER^T:Fgfr1$^{fl/fl}$* mice. A–B: Representative confocal microscopy images of double immunolabeling with NF200 (green; pan-neurofilament marker) and SMI32 (red; nonphosphorylated neurofilament epitope) in the caudal CC of *Plp/CreER^T:Fgfr1$^{fl/fl}$ mice* administered oil (A) or tamoxifen (B). Co-labeled axons appear yellow. C: Quantification of the proportion of SMI32 labeled axons in the CC relative to the total number of axons identified by SMI32 and/or NF200. After 12 wks of cuprizone, significantly fewer axons are immunolabeled for SMI-32 in *Plp/CreER^T:Fgfr1$^{fl/fl}$ mice* administered tamoxifen as compared to oil ($p = 0.0207$; $N = 4$ mice of each condition). Scale bar = 20 μm.

The cuprizone model facilitates identification of specific cellular and molecular interactions that regulate the OP response and capacity to repair chronically demyelinated axons. After removing the cuprizone neurotoxicant, remyelination can be examined more specifically than in other models of chronic demyelination with ongoing disease pathogenesis. The lack of a persistent immune demyelinating component aids in the identification of signaling effects on remyelination processes that are not overshadowed by effects on the immune disease severity. However, studies across multiple experimental models of demyelinating disease are important for analysis in the context of a broader range of pathological features of MS. For example, murine hepatitis virus strain A59 (MHV-A59) infection creates a more complex lesion environment, with pathogenic infection followed by an inflammatory response that clears the virus. Analysis of MHV-A59 lesions in *Fgf2* null mice showed increased oligodendrocyte repopulation of demyelinated lesions (Armstrong et al., 2002). Therefore, the FGF signaling pathway has a robust effect on oligodendrocyte lineage cells in diverse models of demyelinating disease.

The *Plp/CreER^T* line employs sequences of transcriptional control of the mPlp gene that are well characterized to drive expression within the oligodendrocyte lineage from OP cells to mature oligodendrocytes (Fuss et al., 2000; Doerflinger et al., 2003). The *Plp/CreER^T* line was selected to target OP cells leading to remyelination and therefore may be more aligned for the current studies than other lines, such as those driven by NG2 transcription. Accordingly, the present studies demonstrated deletion of *Fgfr1* and *Pdgfra* in approximately a third of NG2 cells (Figs. 3 and 4). This deletion efficiency in the current studies may reflect reduced access of tamoxifen into in the adult CNS, the lower level of PLP transcription in OP cells, or the efficiency of Cre activity with these particular crossed lines. However, the tamoxifen administration effectively revealed significant differences relevant to remyelination in *Plp/CreER^T:Fgfr1$^{fl/fl}$* mice using multiple analysis techniques.

The effect of conditional inducible reduction of FGFR1 on remyelination is dependent upon the actions of endogenous ligands that can activate FGFR1 in this chronic lesion environment. Multiple FGF family ligands are present and/or upregulated during chronic cuprizone demyelination and recovery (Fig. 1, Table 1). FGFR1 expression clusters with expression of FGF2 and FGF12 ligands (Fig. 1). Previous studies support FGF2 among the FGF family members as being a relevant ligand for FGFR1 regulation of OP differentiation. Using neonatal rat OP cultures, we showed that FGF2 inhibition of OP differentiation was disrupted by RNA interference knockdown of FGFR1 but not FGFR2 or FGFR3 (Zhou et al., 2006). FGF12 is not a likely signaling partner with FGFR1 since FGFs 11–14 function as intracellular proteins that act independently of FGFRs (Itoh and Ornitz, 2008). Among the other FGF ligands, only FGF1, 8, 17, and 18 have been reported to regulate OP differentiation in neonatal rat cultures (Fortin et al., 2005; Prendaj et al., 2010). However, members of the FGF8 subfamily (FGF8, 17, and 18) have been reported to act through FGFR3, and not FGFR1 (Fortin et al., 2005). FGF7 interacts only with the IIIb splice variant of FGFR2 (Rubin et al., 1995). Although FGF1 can activate all FGFR forms, FGF1 levels are decreased throughout cuprizone demyelination and recovery stages

Please cite this article as: Zhou, Y.-X., et al., Fibroblast growth factor 1 (FGFR1) modulation regulates repair capacity of oligodendrocyte progenitor cells following chronic demy..., Neurobiol. Dis. (2011), doi:10.1016/j.nbd.2011.08.004

relative to non-treated mice, suggesting that FGF1 is not likely to be a predominant ligand in this lesion environment (Fig. 1).

The similarity of results from analysis of *Fgf2* null mice with the current results in *Plp/CreER^T:Fgfr1$^{fl/fl}$* mice administered tamoxifen provides further support of the potential mechanism of FGF2 signaling through FGFR1 to regulate the efficiency of OP differentiation, oligodendrogenesis, and remyelination. In the contexts of developmental myelination and during remyelination following cuprizone mediated CC demyelination, retroviral lineage tracing showed a significant increase in the frequency of OP differentiation into oligodendrocytes in *Fgf2* null mice compared to wild type mice (Murtie et al., 2005a; Murtie et al., 2005b). Consistent with the current results (Fig. 5), *Fgf2* null mice showed increased oligodendroglial repopulation of lesions following either acute or chronic cuprizone mediated demyelination (Armstrong et al., 2006; Armstrong et al., 2002). This increase of oligodendrocytes was not likely to be due to an effect on OP proliferation as BrdU incorporation was not altered in *Fgf2* null mice (Armstrong et al., 2006; Armstrong et al., 2002), which also corresponds well with our analysis in *Plp/CreER^T:Fgfr1$^{fl/fl}$* mice administered tamoxifen (Fig. 4). Finally, both *Fgf2* null mice and *Plp/CreER^T:Fgfr1$^{fl/fl}$* mice administered tamoxifen show dramatically improved remyelination following chronic cuprizone treatment using both MOG immunolabeling to estimate the area myelinated (Fig. 5) and electron microscopy to measure the proportion of myelinated axons (Fig. 6) (Armstrong et al., 2006; Tobin et al., 2011).

Our studies in *Fgf2* null mice demonstrated an important role of FGF2 signaling on remyelination but the constitutive knockout design could not distinguish among potential cell types involved and could not demarcate the effective disease stage. FGF2 is synthesized by reactive astrocytes and microglia/macrophage cells in demyelinated lesions (Messersmith et al., 2000). In situ hybridization detection of FGF2 demonstrated that relatively low FGF2 levels in the normal adult corpus callosum are markedly increased during acute cuprizone demyelination and maintained at elevated levels during chronic cuprizone demyelination (Armstrong et al., 2006; Armstrong et al., 2002), which was quantitatively shown by the current PCR analysis (Fig. 2). FGF2 inhibition of OP differentiation occurs during acute demyelination and remyelination, as demonstrated by retroviral lineage tracing (Murtie et al., 2005b). However, during acute cuprizone demyelination OP cells are amplified approximately five-fold whereas following chronic cuprizone demyelination only low levels of OP cells are available to carry out remyelination (Armstrong et al., 2006) (Fig. 4G). Therefore, the dramatic effect of FGF2 on remyelination following chronic demyelination may reflect the importance of FGF2 inhibition of OP differentiation when the pool of OP cells is limited.

The tamoxifen inducible approach used to reduce FGFR1 expression now specifically targets the chronic demyelination period and demonstrates a strong effect on remyelination (Figs. 5 and 6). This conditional approach used to reduce FGFR1 expression now also demonstrates that the increased remyelination involves a direct role of FGFR1 in OP cells and oligodendrocytes (Figs. 4 and 5). Although FGF2 may also act through astrocytes to regulate remyelination, preliminary experiments in *GfapCreERT2:Fgfr1$^{fl/fl}$* mice did not show an increase of remyelinated fibers with tamoxifen administration (unpublished data). Importantly, our studies in *Fgf2* null mice showed reduced axon damage compared to *Fgf2* wt mice but could not distinguish direct or indirect effects of FGF2 on axons (Tobin et al., 2011). The current studies (Fig. 7) now demonstrate reduced axon damage that is accomplished through an indirect effect on axons. Specifically, improved axon integrity corresponds with increased oligodendrogenesis and remyelination from reduced FGFR1 expression in oligodendrocyte lineage cells.

The specific examples of FGF2 and FGFR1 impacting remyelination may relate to a more general concept that demyelinated lesions contain signals that inhibit OP differentiation and limit remyelination. Multiple signals in lesions may inhibit oligodendrocyte lineage cells at different stages of maturation and myelin formation. Lingo1 appears to interact with nerve growth factor receptors on oligodendrocytes or axons to inhibit oligodendrocyte process extension and myelination (Bourikas et al., 2010; Lee et al., 2007). Antagonism of Lingo1 promotes OP cell differentiation and remyelination (Mi et al., 2009). Notch1 is also a potent inhibitor of OP cell differentiation and genetic reduction of Notch1 expression in oligodendrocyte lineage cells increases remyelination (Zhang et al., 2009). Interestingly, FGF2 may interact with mastermind-like 1 and Hes5 components of the notch signaling pathway for inhibition of OP differentiation (Zhou and Armstrong, 2007). Lingo1 and Notch1 signaling pathways have not yet been manipulated in the context of a chronic course of demyelination to test effects on repair capacity from a limited pool of OP cells.

Conclusions

The current studies support development of therapeutic strategies to modify the tissue environment following CNS injury or disease to optimize the repair potential of endogenous cells. Specifically, reducing expression of signaling pathways that inhibit OP cell differentiation into oligodendrocytes can dramatically improve remyelination and axon integrity even in a chronic demyelination model. FGF2 and FGFR1 are identified as relevant signaling components limiting remyelination. The pleiotrophic effects of FGF2 create an unfavorable profile for therapeutic development while exploiting the role of specific isoforms of FGFR1 to directly impact oligodendrocyte lineage cell responses may be advantageous.

Acknowledgments

This work was supported by the National Institutes of Health Grant NS39293 (RCA) and National Multiple Sclerosis Society Grant RG3515 (RCA). We appreciate the assistance of Dr. Dennis McDaniel for the electron microscopy studies.

References

Aguirre, A., et al., 2007. A functional role for EGFR signaling in myelination and remyelination. Nat. Neurosci. 10, 990–1002.
Armstrong, R.C., et al., 2006. Endogenous cell repair of chronic demyelination. J. Neuropathol. Exp. Neurol. 65, 245–256.
Armstrong, R.C., et al., 2002. Absence of fibroblast growth factor 2 promotes oligodendroglial repopulation of demyelinated white matter. J. Neurosci. 22, 8574–8585.
Bourikas, D., et al., 2010. LINGO-1-mediated inhibition of oligodendrocyte differentiation does not require the leucine-rich repeats and is reversed by p75(NTR) antagonists. Mol. Cell. Neurosci. 45, 363–369.
Doerflinger, N.H., et al., 2003. Inducible site-specific recombination in myelinating cells. Genesis 35, 63–72.
Fortin, D., et al., 2005. Distinct fibroblast growth factor(FGF)/FGF receptor signaling pairs initiate diverse cellular responses in the oligodendrocyte lineage. J. Neurosci. 25, 7470–7479.
Fuss, B., et al., 2000. Purification and analysis of in vivo-differentiated oligodendrocytes expressing the green fluorescent protein. Dev. Biol. 218, 259–274.
Gould, J., et al., 2006. Comparative gene marker selection suite. Bioinformatics 22, 1924–1925.
Itoh, N., Ornitz, D.M., 2008. Functional evolutionary history of the mouse Fgf gene family. Dev. Dyn. 237, 18–27.
Lee, X., et al., 2007. NGF regulates the expression of axonal LINGO-1 to inhibit oligodendrocyte differentiation and myelination. J. Neurosci. 27, 220–225.
Liu, L., et al., 2010. CXCR2-positive neutrophils are essential for cuprizone-induced demyelination: relevance to multiple sclerosis. Nat. Neurosci. 13, 319–326.
Lobe, C.C., et al., 1999. Z/AP, a double reporter for cre-mediated recombination. Dev. Biol. 208, 281–292.
Lucchinetti, C., et al., 1999. A quantitative analysis of oligodendrocytes in multiple sclerosis lesions. A study of 113 cases. Brain 122, 2279–2295.
Mason, J.L., et al., 2001. Episodic demyelination and subsequent remyelination within the murine central nervous system: changes in axonal calibre. Neuropathol. Appl. Neurobiol. 27, 50–58.
Mason, J.L., et al., 2004. Oligodendrocytes and progenitors become progressively depleted within chronically demyelinated lesions. Am. J. Pathol. 164, 1673–1682.
Messersmith, D.J., et al., 2000. Fibroblast growth factor 2 (FGF2) and FGF receptor expression in an experimental demyelinating disease with extensive remyelination. J. Neurosci. Res. 62, 241–256.

Please cite this article as: Zhou, Y.-X., et al., Fibroblast growth factor 1 (FGFR1) modulation regulates repair capacity of oligodendrocyte progenitor cells following chronic demy..., Neurobiol. Dis. (2011), doi:10.1016/j.nbd.2011.08.004

Mi, S., et al., 2009. Promotion of central nervous system remyelination by induced differentiation of oligodendrocyte precursor cells. Ann. Neurol. 65, 304–315.
Murtie, J.C., et al., 2005a. In vivo analysis of oligodendrocyte lineage development in postnatal FGF2 null mice. Glia 49, 542–554.
Murtie, J.C., et al., 2005b. PDGF and FGF2 pathways regulate distinct oligodendrocyte lineage responses in experimental demyelination with spontaneous remyelination. Neurobiol. Dis. 19, 171–182.
Nait-Oumesmar, B., et al., 2008. The role of SVZ-derived neural precursors in demyelinating diseases: from animal models to multiple sclerosis. J. Neurol. Sci. 265, 26–31.
Pirvola, U., et al., 2002. FGFR1 is required for the development of the auditory sensory epithelium. Neuron 35, 671–680.
Prendaj, E., et al., 2010. FGF-2 is not a prototypic member of the FGF family that regulates oligodendrocyte lineage cells. ASN Neuro. Trans. Am. Soc. Neurochem. PTW07-14.
Redwine, J.M., Armstrong, R.C., 1998. In vivo proliferation of oligodendrocyte progenitors expressing PDGFalphaR during early remyelination. J. Neurobiol. 37, 413–428.
Reich, M., et al., 2006. GenePattern 2.0. Nat. Genet. 38, 500–501.
Rubin, J.S., et al., 1995. Keratinocyte growth factor. Cell Biol. Int. 19, 399–411.
Tallquist, M.D., Soriano, P., 2003. Cell autonomous requirement for PDGFRalpha in populations of cranial and cardiac neural crest cells. Development 130, 507–518.
Tobin, J.E., et al., 2011. Reduced axonopathy and enhanced remyelination after chronic demyelination in fibroblast growth factor 2 (fgf2)-null mice: differential detection with diffusion tensor imaging. J. Neuropathol. Exp. Neurol. 70, 157–165.
Wu, Q.Z., et al., 2008. MRI identification of the rostral–caudal pattern of pathology within the corpus callosum in the cuprizone mouse model. J. Magn. Reson. Imaging 27, 446–453.
Xie, M., et al., 2010. Rostro-caudal analysis of corpus callosum demyelination and axon damage across disease stages refines diffusion tensor imaging correlation with pathological features. J. Neuropathol. Exp. Neurol. 69, 704–716.
Zhang, Y., et al., 2009. Notch1 signaling plays a role in regulating precursor differentiation during CNS remyelination. Proc. Natl. Acad. Sci. U.S.A. 106, 19162–19167.
Zhou, Y.X., Armstrong, R.C., 2007. Interaction of fibroblast growth factor 2 (FGF2) and notch signaling components in inhibition of oligodendrocyte progenitor (OP) differentiation. Neurosci. Lett. 421, 27–32.
Zhou, Y.X., et al., 2006. Retroviral lineage analysis of fibroblast growth factor receptor signaling in FGF2 inhibition of oligodendrocyte progenitor differentiation. Glia 54, 578–590.

Please cite this article as: Zhou, Y.-X., et al., Fibroblast growth factor 1 (FGFR1) modulation regulates repair capacity of oligodendrocyte progenitor cells following chronic demy..., Neurobiol. Dis. (2011), doi:10.1016/j.nbd.2011.08.004